

# Thinned Fiber Bragg Gratings as High Sensitivity Refractive Index Sensor

A. Iadicicco, A. Cusano, *Member, IEEE*, A. Cutolo, R. Bernini, *Member, IEEE*, and M. Giordano

**Abstract**—In this work, the numerical and experimental analysis on the use of thinned fiber Bragg gratings as refractive index sensors have been carried out. Wet chemical etching in a buffered hydrofluoric acid solution was used for sensor fabrication. Experimental characterization for an almost full etched cladding sensor is presented demonstrating good agreement with numerical results and resolutions of  $\approx 10^{-5}$  and  $\approx 10^{-4}$  for outer refractive index around 1.45 and 1.333, respectively.

**Index Terms**—Optical fibers, refractive index measurements, thinned fiber Bragg grating (FBG) sensors.

## I. INTRODUCTION

OPTICAL sensors are very attractive in chemical and biochemical applications due to some unique characteristics such as immunity to electromagnetic interference and aggressive environments, high sensitivity, and fast response. Examples of integrated optical sensors include those utilizing schemes like direct fiber optic reflectometry [1], Mach–Zehnder interferometers, grating couplers, bend loss waveguides or ARROW waveguides [2], and long-period gratings [3].

On the other hand, in the last years, fiber Bragg grating (FBG) sensors have been widely used in many sensing applications including temperature and strain measurements [4]. The advantages of grating-based sensors are well known. High sensitivity, intrinsic codify of the measured parameter in an absolute parameter, multiplexing capabilities, and very low cost are only a few of them. The principle of operation relies on the dependence of the Bragg resonance on effective refractive index and the grating pitch. Since the effective refractive index is not influenced by the external one for standard optical fibers, no sensitivity to external refractive index is expected. However, if fiber cladding diameter is reduced along the grating region, the effective refractive index is significantly affected by external refractive index. As a consequence, shifts in the Bragg wavelength combined with a modulation of the reflected amplitude are expected. This approach has been already used to create grating-based tuneable filters [5]. In this letter, numerical and experimental analysis on the use of thinned FBGs for refractive index measurements is presented. In particular, the three-layer model for the thinned optical fiber has been used to identify the dependence of the effective

refractive index from the external one. From these results, the dependence of the sensor sensitivity in terms of wavelength shift has been analyzed. Sensor fabrication has been carried out by using standard single-mode optical fibers (SMF-28) and wet chemical etching in a buffered hydrofluoric acid (HF) solution. Finally, experimental characterization of the sensor response to external refractive indexes varying in the range 1.333–1.450 has been carried out by using broad-band interrogation and a commercial optical spectrum analyzer.

## II. ANALYSIS AND SIMULATIONS

As is well known, Bragg resonance condition can be expressed as [4]

$$\lambda_B = 2n_{\text{eff}}\Lambda \quad (1)$$

where,  $n_{\text{eff}}$  is the effective refractive index of the fiber,  $\Lambda$  is the grating pitch and  $\lambda_B$  is the reflected Bragg wavelength. In common optical fibers, the effective refractive index  $n_{\text{eff}}$  of the fundamental mode is practically independent from the refractive index of the medium surrounding the cladding. However, if the cladding diameter is reduced,  $n_{\text{eff}}$  shows a nonlinear dependence on the external refractive index, leading to a shift in the reflected wavelength. Different from the common use of this class of sensors for temperature and strain measurements, in this case, only the refractive index  $n_{\text{eff}}$  is affected by measurand changes while the grating pitch was practically unchanged. In order to outline the dependence of the sensor responsivity on cladding diameter and external refractive index,  $n_{\text{eff}}$  in a thinned optical fiber was evaluated by resolving numerically the dispersion equation of a doubly cladding fiber model [6]. The parameters of the optical fiber for the numerical analysis have been chosen according to the SMF-28 standard: core diameter of 8.3  $\mu\text{m}$ , original cladding diameter of 125  $\mu\text{m}$ , core refractive index of 1.460, refractive index difference of 0.36%, and effective refractive index of 1.4588 nm at an operating wavelength of 1550 nm. Fig. 1 shows the nonlinear behavior of  $n_{\text{eff}}$  in a thinned optical fiber versus outer medium refractive index  $n_{\text{out}}$  in the range 1.333–1.4547 at an operating wavelength of 1550 nm for different cladding diameters. Here, the full etching curve is referred to a completely removed cladding and  $D_{\text{clad}}$  is the cladding diameter. For external refractive indexes around 1.333, the guided mode is well confined in the core region, leading to a weak dependence on the outer medium refractive index. As external refractive index increases, higher sensitivity is observed, since the fundamental mode is less confined in the core region leading to an increased interaction with the external medium. In addition, such interaction and as a conse-

Manuscript received September 25, 2003; revised November 27, 2003.

A. Iadicicco, A. Cusano, and A. Cutolo are with the Optoelectronic Division-Engineering Department, University of Sannio, Benevento 82100, Italy (e-mail: a.cusano@unisannio.it).

R. Bernini is with Institute for Electromagnetic Monitoring of Environment (IREA), National Research Council (CNR), 328-80124 Napoli, Italy.

M. Giordano is with Institute of Composite Materials Technology National Research Council (ITMC-CNR), 80-80125 Napoli, Italy.

Digital Object Identifier 10.1109/LPT.2004.824972

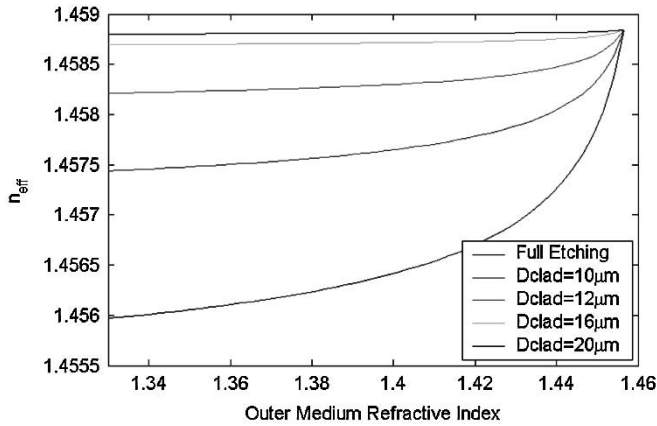


Fig. 1. Effective refractive index of a thinned fiber versus outer medium refractive index for different cladding diameters.

TABLE I  
SENSOR SENSITIVITY IN TERMS OF  $(\Delta\lambda_B/\lambda_B)/(\Delta n_{out}/n_{out})$  FOR  
DIFFERENT CLADDING DIAMETERS AND FOR SEVERAL EXTERNAL  
REFRACTIVE INDEXES

|                  | Full Etching | Dclad=10 $\mu$ m | Dclad=12 $\mu$ m | Dclad=16 $\mu$ m | Dclad=20 $\mu$ m |
|------------------|--------------|------------------|------------------|------------------|------------------|
| $n_{out} = 1.35$ | 4.45         | 2.01             | 7.84e-1          | 1.69e-1          | 3.88e-2          |
| $n_{out} = 1.40$ | 1.04e+1      | 4.79             | 1.99             | 4.03e-1          | 9.28e-2          |
| $n_{out} = 1.45$ | 9.05e+1      | 4.34e+1          | 1.92e+1          | 4.23             | 1.01             |

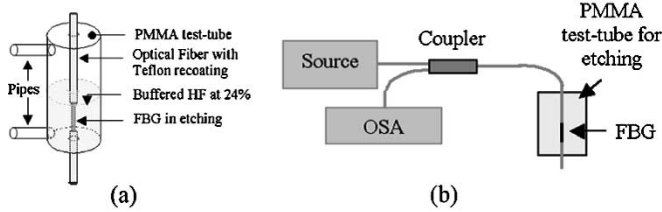


Fig. 2. Experimental setup for sensor fabrication and characterization: (a) etching; (b) optoelectronic measurements.

quence sensor sensitivity increases as cladding diameter is reduced under 20  $\mu$ m. From (1), similar behavior is expected for the Bragg wavelength  $\lambda_B$ . In Table I, sensor sensitivity in terms of  $(\Delta\lambda_B/\lambda_B)/(\Delta n_{out}/n_{out})$  for different cladding diameters and for external refractive indexes is reported.

### III. SENSOR FABRICATION

The fabrication of the thinned FBG sensor was obtained by wet chemical etching in a buffered HF solution [7]. In Fig. 2(a), a schematic diagram of the experimental setup for sensor preparation is shown. The test tube was completely realized in polymethyl methacrylate (PMMA) in order to avoid any chemical interaction between the holder and the HF solution. Cylindrical geometry with base diameter and height of 1 and 3 cm, respectively, was chosen. In the center of the two bases, holes of 1-mm diameter were realized for the positioning of the optical fiber. Here, SMF-28 standard optical fiber was used. The fiber was fixed at the two bases using an epoxy-based resin (EPON 828 by SHELL) and dual functionalities pipes were arranged along the test tube for washing the realized sensor after HF etching and the injection of liquids for further refractive index measurements.

As a sensing element, a commercial 6-mm-long FBG demonstrating a peak reflectance of 95%, a central wavelength of 1549.87 nm, and a bandwidth [full-width at half-maximum (FWHM)] of 0.43 nm was selected. Before the etching, the acrylate buffer coating was removed using chloroform on a length of 10 mm containing the sensing FBG. The remaining part of the optical fiber (still covered with coating) was protected by depositing Teflon with spray-coating technique. HF aqueous solution at 24% was then added to the test tube allowing etching rates of the order of 0.65  $\mu$ m/min at 24 °C (room temperature). In order to obtain the best performances in terms of sensor sensitivity, full cladding stripping was tried and the etching extent fixed at 179 min. When the etching process was completed, HF solution was removed and the test tube filled for 15 min with a basic solution (calcium oxide). The sensor diameter was measured by using scanning electron microscope (SEM) analysis on an additional optical fiber without sensing element fixed to the test tube, opportunely modified to allow the correct positioning of both optical fibers. SEM photograms revealed a thinned diameter of the order of 8.5  $\mu$ m, meaning that almost full etched sensor was obtained.

### IV. EXPERIMENTALS

The optoelectronic setup, involved for both fabrication process monitoring and for further refractive index measurements, is shown in Fig. 2(b). It comprises a broad-band superluminescent diode (2 mW) operating at 1550 nm with 40-nm FWHM, a directional 3-dB coupler to collect the reflected spectrum from the sensor head, and an optical spectrum analyzer for spectral measurements.

Grating spectra measurements have been carried out by recording the reflected spectrum from the sensing grating for each liquid sample. Centroid analysis was used for Bragg wavelength identification allowing resolution in wavelength of the order of 10 pm over the whole investigated range.

During the etching process, after 170 min corresponding to a cladding diameter of approximately 20  $\mu$ m, a diminution of both the Bragg wavelength and peak reflectance, was observed. The first effect is related to the monotonic effective refractive index decreasing due to the extent of the etching procedure. Indeed, the aqueous HF solution refractive index is similar to water index (1.3330) while the original cladding one is around 1.4547. A 2.92-nm final Bragg wavelength shift was recorded; this value is very close to that obtained from numerical analysis for an 8.5- $\mu$ m etched sensor (2.95 nm).

The second effect related to peak reflectance diminution could be attributable to the etching-induced multimodal propagating conditions along the etched region. This effect leads to a diminution of the fundamental mode power and then of the grating-induced coupling. A peak reflectivity reduction of 30% was observed. This effect, maximum for external refractive index around 1.33 decreases significantly in the range of maximum sensitivity of the proposed sensor around 1.45, where only monomodal propagation is allowed. In order to characterize the sensor sensitivity to refractive index changes, aqueous glycerine solutions at different concentrations were used as outer media. A commercial Abbe refractometer with

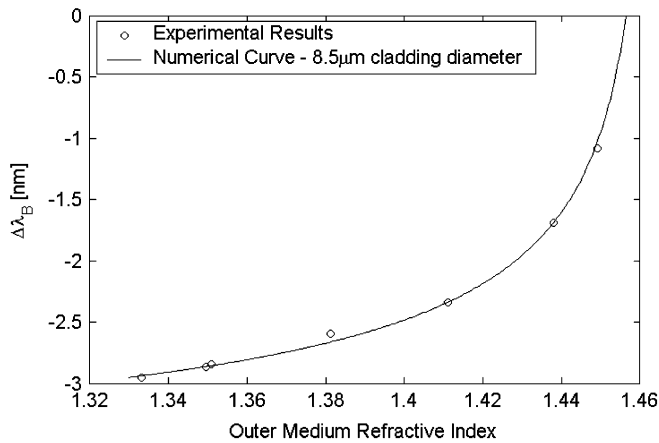


Fig. 3. Wavelength shift of the reflected signal of the thinned Bragg filter (dotted line) and the numerical curve (solid line) with cladding diameter of 8.5  $\mu\text{m}$  versus external medium.

a resolution of  $10^{-4}$  was used for reference characterization. By adding glycerine concentrations, liquids with refractive indexes varying in the range 1.3330–1.4500 were obtained. Fig. 3 shows the measured wavelength shift as function of refractive index at room temperature (dotted line) together with the numerical one obtained in the case of 8.5- $\mu\text{m}$  etched sensor (solid line). Here,  $\Delta\lambda_B$  represents the difference between the before-etching Bragg wavelength and the actual one. Good agreement is obtained. From these results, it is evident how thinned FBG sensor sensitivity is lower in respect of long period grating (LPG) sensors [8], [9]. Although, thinned FBG sensors exhibit lower sensitivity in respect to LPG sensors, their performances in terms of refractive index resolution are comparable with relatively lower cost instrumentation. In fact, for FBG demodulation, several low-cost FBG interrogation units with high performances (1-pm resolution around 1550 nm) have been proposed in the past decade [10]. On the other hand, for the demodulation of LPG sensors, only spectral analysis with lower resolution and higher costs have been proposed. From these results and in the case of interrogation units able to discriminate wavelength shifts with a resolution of 1 pm at 1550 nm [10], refractive index resolutions of  $\approx 10^{-5}$  and  $\approx 10^{-4}$  are possible for almost full etched sensor and for outer refractive index around 1.45 and 1.333, respectively. In addition, the diminution in the FBG peak reflectivity due to the

etching process is not able to influence the system performance for the most interrogation units proposed in literature.

## V. CONCLUSION

A simple and low-cost all-fiber refractive index sensor based on thinned FBGs, with performances adequate to the actual state of the art, has been presented. Numerical analysis, involving the investigation of doubly cladding fibers, was useful for the identification of sensor sensitivity dependence on cladding diameter and outer refractive index. A simple and low-cost procedure involving wet chemical etching in a buffered HF solution has been carried out for sensor preparation. Experimental characterization of the sensor response to refractive index changes has been carried out by using broad-band interrogation and spectral measurements. Resolutions of  $10^{-5}$  and  $10^{-4}$  are possible for the outer refractive index around 1.45 and 1.333, respectively, if easily available wavelength discriminators with a minimum detectable of 1 pm are used. In addition, fiber operation allows accurate measurements not affected by alignment problems typical of waveguide based refractive index sensors.

## REFERENCES

- [1] A. Cusano, A. Cutolo, M. Giordano, and L. Nicolais, "Optoelectronic refractive index measurements: Applications to smart polymer processing," *IEEE Sensors J.*, vol. 3, pp. 781–787, Dec. 2003.
- [2] R. Bernini, S. Camponiano, and L. Zeni, "Silicon micromachined hollow optical waveguides for sensing applications," *IEEE J. Select. Topics Quantum Electron.*, vol. 8, pp. 106–110, Jan./Feb. 2002.
- [3] H. J. Patrick, A. D. Kersey, and F. Bucholtz, "Analysis of the response of long period fiber gratings to external index of refraction," *J. Lightwave Technol.*, vol. 16, pp. 1606–1612, Sept. 1998.
- [4] A. D. Kersey, M. A. Davis, H. J. Patrick, M. LeBlac, K. P. Koo, C. G. Askins, M. A. Putnam, and E. J. Friebele, "Fiber grating sensors," *J. Lightwave Technol.*, vol. 15, pp. 1442–1463, Aug. 1997.
- [5] H. Kumazaki, Y. Yamada, H. Nakamura, and S. I. K. Hane, "Tunable wavelength using a Bragg grating fiber thinned by plasma etching," *IEEE Photon. Technol. Lett.*, vol. 13, pp. 1206–1208, Nov. 2001.
- [6] M. Monerie, "Propagation in doubly clad single-mode fibers," *IEEE J. Quantum Electron.*, vol. QE-18, pp. 535–542, Apr. 1982.
- [7] E. R. Lyons and H. P. Lee, "Demonstration of an etched cladding fiber Bragg grating filter with reduced tuning force requirement," *IEEE Photon. Technol. Lett.*, vol. 11, pp. 1626–1628, Dec. 1999.
- [8] X. Shu, L. Zhang, and I. Bennion, "Sensitivity characteristics of long-period fiber gratings," *J. Lightwave Technol.*, vol. 20, pp. 255–266, Feb. 2002.
- [9] M. N. Ng, Z. Chen, and K. S. Chiang, "Temperature compensation of long-period fiber grating for refractive-index sensing with bending effect," *IEEE Photon. Technol. Lett.*, vol. 14, pp. 361–362, Mar. 2002.
- [10] R. M. Measures, *Structural Monitoring with Fiber Optic Technology*, London, U.K.: Academic, 2001.